

## Magnetotunneling spectroscopy in a double-barrier heterostructure: Observation of incoherent resonant-tunneling processes

C. H. Yang,\* M. J. Yang, and Y. C. Kao

Central Research Laboratories (Mail Stop 154), Texas Instruments, Inc., P.O. Box 655 936, Dallas, Texas 75265

(Received 10 April 1989)

We report striking magneto-oscillations in the current-voltage characteristics of a double-barrier resonant-tunneling structure under longitudinal magnetic field. We have identified, for the first time, inter-Landau-level resonant tunneling with Landau-level indices changed by as large as six, two distinct LO-phonon-emission-assisted resonant tunneling, and a combination of the two. The voltage-to-energy conversion is experimentally calibrated, which makes tunneling spectroscopy possible. Our experiment is a manifestation of the two-dimensionality of the source electrons.

Vertical transport through artificial structures has been under intense investigation since the pioneering work of Chang, Esaki, Tsu.<sup>1</sup> Among the various structures, the double-barrier (DB) heterostructure has demonstrated high-speed switching capability<sup>2</sup> and has stimulated numerous theoretical and experimental studies on the physics of resonant tunneling (RT). In the original Tsu-Esaki picture,<sup>3</sup> the electron tunneling transmission coefficient is resonantly enhanced when the electron's longitudinal energy coincides with the bottom of the quantum-well subbands, and the transverse momentum ( $k_{\perp}$ ) is conserved. Then, as the device is biased through resonance, the current-voltage ( $I$ - $V$ ) characteristics would show a negative differential resistance (NDR). Experimental studies on DB heterostructures have been performed almost exclusively under the assumption that the source electrons are three dimensional. It has been shown by magnetotunneling experiments that under a longitudinal magnetic field<sup>4</sup> ( $B_{\parallel}$ , parallel to current) the quantum-well electrons are of two-dimensional (2D) nature, even for thin tunneling barriers. Together with data taken under a transverse magnetic field  $B_{\perp}$ ,<sup>5</sup> the  $I$ - $V$  characteristics of DBRT structures can be *qualitatively* explained by considering tunneling as occurring through a 3D-2D-3D system. However, many features of such  $I$ - $V$  characteristics still cannot be quantitatively calculated, and an accurate description of the DBRT phenomenon has yet to be developed. As an example, the inclusion of scattering-assisted tunneling processes will alter the  $I$ - $V$  characteristics, since either elastic or inelastic scattering can relax the constraints imposed by the conservation laws.<sup>6</sup> Furthermore, the uncertainties in the band bending make an accurate assignment of the energy scale, necessary to perform tunneling spectroscopy, difficult in RT structures. A self-consistent band-bending calculation predicts the existence of a 2D accumulation layer<sup>7</sup> at the emitter side and a depletion region at the collector side under bias. However, both have yet to be experimentally confirmed. In fact, without detailed understanding of the RT processes, theoretical calculations of band-bending and  $I$ - $V$  characteristics become arbitrary.

In this paper, we report the tunneling spectroscopy of a DBRT heterostructure, where the source electrons are *two-dimensional* electron gas at the near side of the first barrier. As a result of the two dimensionality of the source electrons, the features of our  $I$ - $V$  characteristics are drastically different in many respects from the case where the emitter electrons are three dimensional. We find that the conversion from the applied voltage to energy can be experimentally calibrated, which makes possible the identification of both the elastic- and inelastic-scattering-assisted tunneling mechanisms. In the presence of  $B_{\parallel}$ , we find that both the peak and the valley currents decrease as  $B_{\parallel}$  is increased, and the NDR *disappears* for  $B_{\parallel} \geq 3.5$  T. The valley current shows magneto-oscillations, which we interpret as arising from a combination of elastic and inelastic tunneling processes. Electrons can tunnel from a Landau level in the 2D accumulation layer into a Landau level of the quantum well with different indices, where the change of indices from 0 up to 6 is observed for the first time. The total energy of such elastic, but incoherent tunneling processes is conserved, but not the transverse momentum  $k_{\perp}$ . In addition, we find that when the energy separation between the Landau levels is equal to either the GaAs-like ( $\hbar\omega_{LO_1}$ ) or AlAs-like ( $\hbar\omega_{LO_2}$ ) LO-phonon energies in the  $\text{Al}_{0.37}\text{Ga}_{0.63}\text{As}$  barriers, the resonant-tunneling current is also enhanced. Most strikingly, we observe that the above LO-phonon-assisted, inelastic tunneling can occur between Landau levels with different indices. In contrast, the differential conductance just before NDR does not show magneto-oscillations under  $B_{\parallel}$ , different from what has been reported in the case of degenerate 3D source electrons.<sup>4</sup> On the other hand, we find that when a transverse magnetic field  $B_{\perp}$  is applied, the biasing position of the NDR shifts higher. The voltage shift agrees well with a calculation based on a perturbation theory which will be discussed below. The peak-to-valley current difference degrades only slightly by  $\approx 20\%$  when  $B_{\perp} = 9$  T, much less than what has been found in the case of 3D source electrons.<sup>5</sup> Our study therefore identifies two in-

coherent RT processes, and both of which contribute to the valley current.

Our experiments were performed on GaAs/Al<sub>x</sub>Ga<sub>1-x</sub>As heterostructures grown by molecular-beam epitaxy on *n*<sup>+</sup>-type GaAs substrates. The sample structure consists of a thick (1-μm) *n*<sup>-</sup>-type region (Si doped to 1×10<sup>15</sup>/cm<sup>3</sup>), a 50-Å undoped Al<sub>0.37</sub>Ga<sub>0.63</sub>As barrier, a 70-Å GaAs quantum well, a second 50-Å undoped Al<sub>0.37</sub>Ga<sub>0.63</sub>As barrier, and a thick (0.5-μm) *n*<sup>+</sup>-type GaAs cap layer. It is established that a wide *n*<sup>-</sup>-type region forms a two-dimensional accumulation layer at the first barrier.<sup>8</sup> The devices are defined by standard photolithography and mesa etching techniques. Ohmic contacts to the top and to the substrate are made by NiGe/Au alloying. We report results taken from a device with an area of 5×5 μm<sup>2</sup>, and the representative features are similar in all devices. A standard ac modulation technique is employed to measure the differential conductance  $G=dI/dV$ . The voltage is measured with the use of a pseudo-four-terminal technique, and the current is taken from a 1 Ω resistor. At room temperature, the NDR is clearly observed at 0.18 V. A broad replica peak<sup>9</sup> in the valley current (near 0.3 V) appears at ≈100 K, and becomes more pronounced at lower temperatures. The *I-V* and the *G-V* characteristics at 4.2 K under several different  $B_{\parallel}$  are shown in Fig. 1. When  $B_{\parallel}$  is zero, the first and the second NDR occur at 0.195 and 0.49 V, respectively. In the first NDR region, 0.195 ≤ *V* ≤ 0.23 V, the *I-V* curves display a shoulderlike structure due to oscillations, and no hysteresis was observed. The first peak current decreases gradually from 1.12 mA at  $B_{\parallel}=0$  to 0.5 mA as  $B_{\parallel}$  is increased to 9 T. The first NDR disappears when  $B_{\parallel} \geq 3.5$  T. The valley current shows discernible oscillations when  $B_{\parallel} > 0$ , and the features are more apparent in the *G-V* characteristics.

To determine the origin of these magneto-oscillations, the *G-V* characteristics are taken for various  $B_{\parallel}$  from 0 to 9 T with an increment of 0.117 T. In Fig. 2, we summarize the data by plotting the dips in the  $dI/dV$  oscillations as a function of the slow ramping (≈0.1 mV/sec) dc bias. The positions of the peaks and valleys of the NDR are indicated by triangles (Δ), and other dips are represented by “●” and “○,” with a decreasing signal strength. It is apparent that the data group themselves into four sets of curves, each converging to a voltage when  $B_{\parallel} \rightarrow 0$ , as indicated by  $\Delta E_1$ ,  $\Delta E_2$ ,  $\Delta E_3$ , and  $\Delta E_4$  in Fig. 2. The first set consists of several almost equally spaced lines, which are labeled by  $\Delta n=0,1,2,3 \dots$  on the top of Fig. 2. The second and the third sets are replicas of the first one, and the lines are labeled by  $\Delta n_{\text{GaAs}}$  and  $\Delta n_{\text{AlAs}}$ , respectively.

We explain the data as follows. Figure 3 plots the schematic energy-band diagram of our DBRT structure when biased beyond the resonance. The emitter Fermi level  $E_{F,E}$  is aligned with that of the 2D accumulation layer at the near side of the first barrier.<sup>9</sup> The subband minima are denoted by  $E_0$ ,  $E'_0$ , and  $E'_1$ , and the bias voltage *V* is applied between the collector Fermi level  $E_{F,C}$  and  $E_{F,E}$ . Since the collector is highly degenerate ( $E_{F,C} - E_c \approx 80$  meV,  $E_c$  being the conduction-band

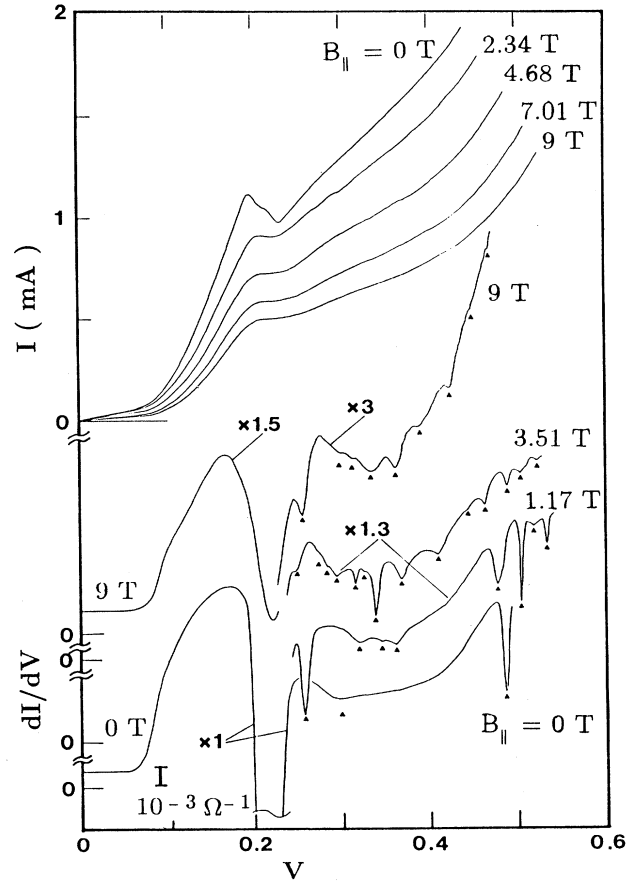


FIG. 1. *I-V* and *G-V* characteristics of the device under various magnetic fields at 4.2 K.

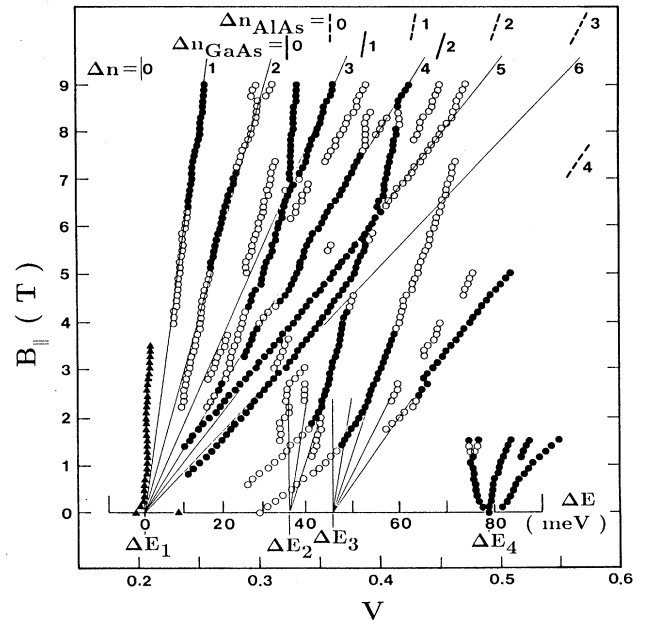


FIG. 2. The bias positions, at which the dips in the *G-V* curves are observed, are plotted as a function of  $B_{\parallel}$ . The  $\Delta E$  scale is obtained experimentally, see context.

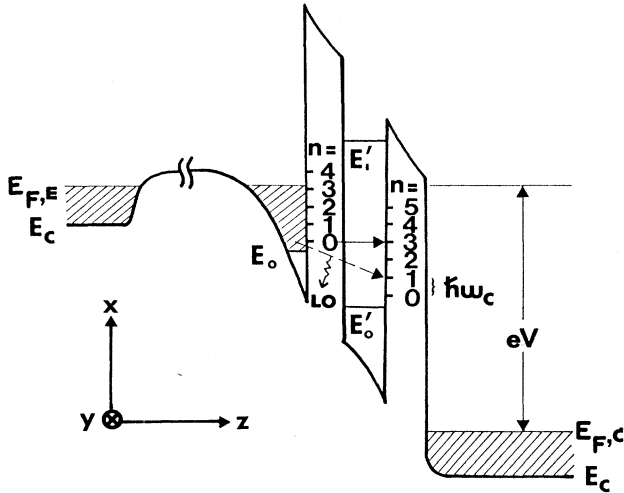


FIG. 3. The schematic conduction-band energy diagram of the device when biased in the valley current region, under magnetic field parallel to the  $z$  direction. Landau levels with indices from 0 to 5 are shown as short segments for both the source electrons and the metastable states in the quantum well. The arrow with a solid line indicates the elastic inter-Landau-level resonant tunneling ( $\Delta n=3$  is shown as an example), and the one with a dashed line indicates the phonon-emission-assisted resonant tunneling ( $\Delta n=2$ , i.e.,  $2\hbar\omega_c = \hbar\omega_{LO}$ ).

minimum) the voltage drop on the collector side is negligible for this discussion. The transverse energy of 2D electrons in both the accumulation layer and the quantum well is further quantized by  $B_{\parallel}$  into Landau levels, labeled by  $n=0, 1, 2, \dots$ , as shown in Fig. 3. The resonant-tunneling probability of accumulation electrons in different Landau levels to first order is the same because electrons with higher Landau-level index have the same *longitudinal* kinetic energy. However, when  $\Delta E = E_0 - E'_0 = \Delta n \hbar\omega_c$  ( $\omega_c$ , cyclotron frequency, is  $eB_{\parallel}/m^*$ , where  $m^*$  is the effective mass), electrons in the accumulation layer can tunnel into a Landau level of the quantum well with a different index, i.e.,  $\Delta n = 1, 2, 3, \dots$ , as shown in Fig. 2. Such transitions are elastic, phase-incoherent resonant-tunneling processes. Since the total energy is conserved, the change in the transverse kinetic energy and momentum must be transferred to the longitudinal direction via elastic scattering, e.g., impurity scattering. As shown in Fig. 2, as many as six index-nonconserving processes are observed for the first time. In our case, the longitudinal tunneling probability is the same for two-dimensional source electrons, where sharp features are expected. In the case of 3D source electrons, the spread of longitudinal energy ( $\sim E_{F,E}$ ) makes these features less pronounced if  $E_{F,E}$  is comparable to or greater than  $\hbar\omega_c$ . For most reported experimental works the emitter is heavily doped, therefore  $E_{F,E}$  is several tens of meV, while  $\hbar\omega_c$  is only 1.73 meV at 1 T.

Magneto-oscillations of the tunneling conductance, either at the peak or in the valley current regime, have been attributed to the two-dimensional accumulation

electrons.<sup>10</sup> However, here we demonstrate that the oscillation actually comes from two dimensionality of the quantum-well metastable states. The nature of resonant enhancement of the tunneling current through the resonant states (Landau levels) of the quantum well in DB structures is distinctly different from the case of single-barrier tunneling.<sup>8</sup> Resonant enhancement allows tunneling to occur mainly within a narrow energy channel, while the self-consistent band bending is responsible for the magneto-oscillations in single-barrier tunneling experiments. An observation of magneto-oscillation only indicates that the quasibound states in the quantum well are still two dimensional, since it doesn't matter whether the source electrons are two dimensional or not. The oscillations, claimed<sup>10</sup> periodic in  $1/B_{\parallel}$ , are therefore not related to two-dimensional electron density at the accumulation layer. In fact, the oscillations would not be strictly periodic in  $1/B_{\parallel}$ , as will be discussed below.

Our data also show striking structures due to phonon emission during the tunneling process. When the energy between any two quantum-well Landau levels differs by either  $\hbar\omega_{LO_1}$  or  $\hbar\omega_{LO_2}$ , tunneling current is enhanced. Due to energy conservation, such enhancement occurs when  $\Delta E = \Delta n_{\text{GaAs}} \hbar\omega_c + \hbar\omega_{LO_1}$ , for the emission of the GaAs-like LO phonons in  $\text{Al}_{0.37}\text{Ga}_{0.63}\text{As}$ , and when  $\Delta E = \Delta n_{\text{AlAs}} \hbar\omega_c + \hbar\omega_{LO_2}$ , for the AlAs-like LO phonons.<sup>11</sup> We observed strong signals that are attributed to  $\Delta n_{\text{GaAs}} = 0, 2$ , and  $\Delta n_{\text{AlAs}} = 1, 2, 4$ , where  $\Delta n_{\text{GaAs}} = 1$  and  $\Delta n_{\text{AlAs}} = 0$  and 3 are not substantiated. The data which converge to  $\Delta E_4$  in Fig. 2 are due to the first excited resonant state in the quantum well.

The linearity of the curves implies that the relative energy separation between  $E_0$  and  $E'_0$  is approximately linearly proportional to  $V$ , i.e.,  $\Delta E = E_0 - E'_0 = \alpha e(V - 0.205 \text{ V})$ . Here, 0.205 V is the voltage position of  $\Delta E_1$ , as indicated in Fig. 2. The proportionality constant  $\alpha$  can be experimentally obtained by taking the energy spacings between oscillations at 9 T in the  $\Delta n$  group in Fig. 2 to be 15.57 meV ( $=\hbar\omega_c$ ). We find  $\alpha$  varies slowly from 0.31 to 0.26 in the biasing range from 0.205 to 0.534 V. This experimentally calibrated energy  $\Delta E$  is also shown in Fig. 2. The first excited state is therefore measured to be 79 meV above  $E'_0$ , in reasonable agreement with that calculated under zero-bias condition. Using this calibrated energy scale, the phonon energies  $\hbar\omega_{LO_1}$  and  $\hbar\omega_{LO_2}$  are found within our experiment accuracy to be  $\Delta E_2 = 37 \pm 2 \text{ meV}$  and  $\Delta E_3 = 46 \pm 2 \text{ meV}$ , respectively, similar to that observed by Raman scattering.<sup>11</sup> Considering the DBRT structure as a voltage divider, where the two barriers are put in series,  $\alpha$  should be close to one-half since the barriers are of the same thickness. The uncertainty of the film thicknesses is within 10% and cannot account for such a large deviation in  $\alpha$ . We attribute the deviation to the fact that a population of electrons in the quantum well can partially screen the electric field across the first tunneling barrier, thereby causing  $\alpha$  to be smaller than one-half.

The rising part of the  $I$ - $V$  characteristics ( $0.08 \leq V \leq 0.2 \text{ V}$ ) becomes narrower with increasing  $B_{\parallel}$ , and the

current simply gradually decreases without showing magneto-oscillations. The decrease of the current and the disappearance of the NDR can be attributed to either discrete (Landau-level) density of states, or a longer tunneling path at a higher  $B_{\parallel}$  and the accompanying higher scattering probability. The observed Landau-level width in the valley current does not show a  $\sqrt{B}$  dependence, which is characteristic of broadening resulting from short-range scattering.<sup>12</sup> Instead, the width decreases only slightly as  $B_{\parallel}$  is increased. The relation between the original Landau-level width (which comes from electronic properties in the transverse direction) and the width measured in such conductance oscillation versus bias measurements (longitudinal transport) is not clear. One complication comes from the fact that transport measurements (current) require that electrons scatter to other Landau levels with different indices.

As shown in Fig. 2, the phonon-emission-assisted curves bend at low  $B_{\parallel}$ , and the signal is significantly weaker and broadened. This feature is represented by the hollow circles in Fig. 2 for  $B_{\parallel}$  below 2 T; also see the lowest line in Fig. 1 for comparison. We argue that at low  $B_{\parallel}$  a broad and weak dip in conductance does not represent a perfectly aligned resonant condition, since tunneling current is an integration of the tunneling probability, density of states and population of initial-final states over the initial energy spread. In the case of low  $B_{\parallel}$ , the Landau-level spacing is much less than the level broadening itself, which makes the resonant enhancement not significant, and the position of the “peak” not well defined. The crossover between phonon-assisted and direct inter-Landau-level transitions shows the crossing and anticrossing phenomena, which are still under investigation.

When the magnetic field  $B_{\perp}$  is applied perpendicular to the direction of the current, the  $I$ - $V$  and  $G$ - $V$  characteristics do not show magneto-oscillations. As shown in Fig. 4, the first resonance shifts to higher biasing voltages with increasing  $B_{\perp}$ , while the difference between the peak and the valley current at resonance only decreases from  $\approx 120 \mu\text{A}$  to  $\approx 100 \mu\text{A}$  as  $B_{\perp}$  goes from zero to 9 T. Under  $B_{\perp}$ , an electron in the source accumulation layer with momentum  $(k_{\parallel}, k_x, k_y)$  can only tunnel into the double-barrier quantum well with a momentum  $(k_{\parallel}, k_x + eB\langle z\rangle/\hbar, k_y)$ , where  $\langle z \rangle$  is the averaged value of  $z$ . The shift in the transverse momentum scales up the voltage required to completely destroy the resonant tunneling. The inset of Fig. 4 plots the experimental peak-current energy position  $\Delta E$  versus  $B_{\perp}$ . Also drawn in the inset is our calculated dependence. A first-order perturbation calculation for  $\Delta E$  perturbed by  $B_{\perp}$  gives<sup>13</sup>  $\Delta E \approx e^2 B^2 \langle z^2 \rangle / 2m^* + 2eB \langle z \rangle \hbar k_{F,E} / 2m^*$ , where  $\langle z^2 \rangle$  is the averaged value of  $z^2$ , and  $k_{F,E}$  is the Fermi wave vector of the source 2D electrons. Taking  $\langle z^2 \rangle \approx \langle z \rangle^2$ , a least-squares fit gives  $\langle z \rangle \approx 208 \text{ \AA}$ , and  $E_{F,E} - E'_0 \approx 25 \text{ meV}$ , in reasonable agreement with our sample structure.

In conclusion, we have reported the first magnetotunneling spectroscopy on the valley current of a DBRT structure. The energy scale is experimentally determined from the  $B_{\perp}$  versus  $V$  fan diagram, therefore the previous

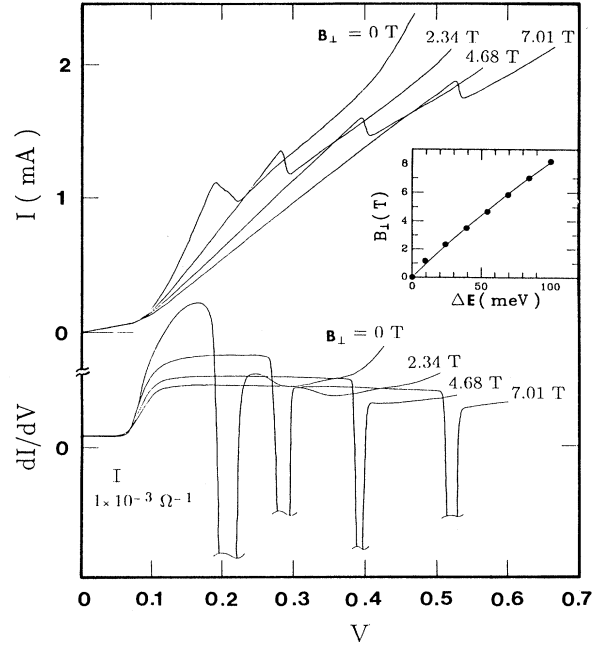


FIG. 4. The  $I$ - $V$  and  $G$ - $V$  characteristics under  $B_{\perp}$ . The inset shows the experimentally calibrated energy shift as a function of  $B_{\perp}$  (dots), and the calculated result using a perturbation theory (solid line).

difficulty of obtaining the energy scale in such DBRT structures is avoided. The source electrons in our sample are two dimensional, which is made possible by lightly doping the semiconductor buffer layer. The new features in our data, different from other cases where source electrons are three dimensional, are (1) sharp structures observed in valley current under  $B_{\parallel}$ , (2) two incoherent RT processes are identified, i.e., inter-Landau-level tunneling ( $\Delta n = 0$  to 6 in Fig. 2) and phonon-assisted tunneling ( $\Delta n_{\text{GaAs}} = 0$  to 2 and  $\Delta n_{\text{AlAs}} = 0$  to 4 shown in Fig. 2), (3) the peak-valley current difference is substantially reduced by  $B_{\parallel}$ , and (4) the peak-valley current difference is insensitive to  $B_{\perp}$ . The observation of the sharp features is mainly due to the two dimensionality of source electrons, since their longitudinal kinetic energy and therefore the RT probability and their contribution to the tunneling current, to first order, are the same. The oscillations observed would be smeared out in the case of 3D source electrons because the spread in the longitudinal energy is as large as the bulk Fermi energy. Our observation of inter-Landau-level elastic scattering also indicates that it is possible to make use of such RT devices for a far-infrared light source, emission energy  $\hbar\omega_c$  being tunable by a longitudinal magnetic field. We expect a population inversion between Landau levels, because hot electrons can be conveniently supplied by biasing current, while the electrons in the lower Landau levels can resonantly tunnel out at a fast escape rate.

We thank B. Bate for encouragement and K. K. Choi for helpful conversations. We are indebted to J. H. Luscombe for his critical reading of the manuscript and informative discussions.

- \*Present address: Department of Electrical Engineering, University of Maryland, College Park, MD 20742.
- <sup>1</sup>L. L. Chang, L. Esaki, and R. Tsu, *Appl. Phys. Lett.* **24**, 593 (1974).
- <sup>2</sup>See, e.g., T. C. L. G. Sollner, W. D. Goodhue, P. E. Tannenwald, C. D. Parker, and D. D. Deck, *Appl. Phys. Lett.* **43**, 588 (1983).
- <sup>3</sup>R. Tsu and L. Esaki, *Appl. Phys. Lett.* **22**, 562 (1973).
- <sup>4</sup>E. E. Mendez, L. Esaki, and W. I. Wang, *Phys. Rev. B* **33**, 2893 (1986); V. J. Goldman, D. C. Tsui, and J. E. Cunningham, *ibid.* **36**, 7635 (1987).
- <sup>5</sup>S. Ben Amor, K. P. Martin, J. J. L. Rascol, R. J. Higgins, A. Torabi, H. M. Harris, and C. J. Summers, *Appl. Phys. Lett.* **53**, 2540 (1988).
- <sup>6</sup>A. D. Stone and P. A. Lee, *Phys. Rev. Lett.* **54**, 1196 (1985); L. I. Glazman and R. I. Shekhter, *Solid State Commun.* **66**, 65 (1988); N. S. Wingreen, K. W. Jacobsen, and J. W. Wilkins, *Phys. Rev. Lett.* **61**, 1396 (1988).
- <sup>7</sup>H. Ohnishi, T. Inata, S. Muto, N. Yokoyama, and A. Shibamoto, *Appl. Phys. Lett.* **49**, 1248 (1986).
- <sup>8</sup>This is a direct result of the self-consistent band bending. See related works in single-barrier structures, e.g., T. W. Hickmott, *Phys. Rev. B* **32**, 6531 (1985); E. Bockenhoff, K. v. Klitzing, and K. Ploog, *ibid.* **38**, 10120 (1988).
- <sup>9</sup>V. J. Goldman, D. C. Tsui, and J. E. Cunningham, *Phys. Rev. B* **35**, 9387 (1987).
- <sup>10</sup>M. L. Leadbeater, E. S. Alves, L. Eaves, M. Henini, O. H. Hughes, A. Celeste, J. C. Portal, G. Hill, and M. A. Pate, *Phys. Rev. B* **39**, 3438 (1989); S. Bending, C. Zhang, K. v. Klitzing, and K. Ploog, *ibid.* **39**, 1097 (1989); S. Ben Amor, K. P. Martin, J. J. L. Rascol, R. J. Higgins, R. C. Potter, A. A. Lakhani, and H. Hier, *Appl. Phys. Lett.* **54**, 1908 (1989).
- <sup>11</sup>B. Jusserand and J. Sapriel, *Phys. Rev. B* **24**, 7194 (1981); J. A. Kash, S. S. Jha, and J. C. Tsang, *Phys. Rev. Lett.* **58**, 1869 (1987).
- <sup>12</sup>T. Ando and Y. Uemura, *J. Phys. Soc. Jpn.* **36**, 959 (1974).
- <sup>13</sup>F. Stern, *Phys. Rev. Lett.* **21**, 1687 (1968).